International Journal of Control, Automation and Systems 14(2) (2016) 389-399
http://dx.doi.org/10.1007/s12555-014-0324-9
ISSN:1598-6446 eISSN:2005-4092
http://www.springer.com/12555

Control of a Laboratory 3-DOF Helicopter: Explicit Model Predictive Approach

Ju Zhang*, Xinyan Cheng, and Jiaqi Zhu

Abstract: A helicopter flight control system is a typical multi-input, multi-output system with strong channel-coupling and nonlinear characteristics. This paper presents an explicit model predictive control (EMPC) for attitude regulation and tracking of a 3-Degree-of-Freedom (3-DOF) helicopter. A state-space representation of the system is established according to the characteristics of each degree-of-freedom motion. Multi-Parametric Quadratic Programming (MPQP) and online computation processes for explicit model predictive control and controller design for a 3-DOF helicopter are discussed. The controller design for set-point regulation and tracking time-varying reference signals of a 3-DOF helicopter are presented respectively. Numerical study of explicit model predictive control for attitude regulation and tracking of a 3-DOF helicopter are conducted. A hardware-in-the-loop experimental study of explicit model predictive control of a 3-DOF helicopter is made. To analyze the performances of an EMPC controlled helicopter system, an Active Mass Disturbance System and manual interference are considered in comparison with PID scheme. Numerical simulation and HIL experimental studies show that explicit model predictive control is valid and has satisfactory performance for a 3-DOF helicopter.

Keywords: Explicit model predictive control, hardware in the loop, regulation, tracking, 3-DOF helicopter.

1. INTRODUCTION

A 3-Degree-of-Freedom (3-DOF) helicopter system is a high-order, nonlinear and strongly coupled experiment platform, which is suitable for real flight simulation and control algorithm validation. At present, many universities and research institutes are using this system for control theory research and verification [1]. In recent years, considerable attention has been given to the analysis and control of helicopters. A state feedback robust controller method based on the output-regulation theory and signal compensation is proposed in literature [2]. This method permits the existence of unknown uncertainties and external disturbances in the helicopter system. Dynamic state feedback is applied to 3-DOF helicopter control and the controller is designed using nonlinear structure algorithm [3]. Three identification methods are discussed to improve the control performance. Design and flight -testing of various h-infinity controllers are summarized [4] and the H_∞ controllers are designed using linearization extracted from a new nonlinear model of the Bell 205 helicopter. This approach effectively solves the uncertainty of the MIMO system. A dynamic sliding mode control approach [5] is proposed for attitude stabilization of a nonlinear helicopter model in vertical flight. While retaining the basic robustness associated with sliding model control policies, the proposed approach also results in smoothed input trajectories and state variable responses. Although these methods usually obtain satisfactory control performance under certain circumstances, they are unable to cope with the problems of actuator constraints, states and output constraints effectively. Moreover, these methods mainly focused on the set-point regulation problem of a helicopter, and little research work has been done on tracking time-varying reference signals.

Model Predictive Control (MPC) is one of the most effective methods to deal with multi-variable constrained optimal control problems and is now widely used with great economic and social benefits in the field of industrial process control, such as the petrol and chemical industries [6]. However, the traditional (implicit) model predictive control system, which is based on the on-line repeated solving of the optimization problem with moving horizon, is typically only used to solve problems with slow dynam-

Manuscript received August 21, 2014; revised Febrary 5, 2015 and March 24, 2015; accepted April 12, 2015. Recommended by Associate Editor Won-jong Kim under the direction of Editor PooGyeon Park. The authors would like to thank the anonymous reviewers for their valuable comments and suggestions that help improve the manuscript. The authors would also like to thank the Automatic Control Laboratory of ETHZ for providing MPT, a Matlab toolbox for multi-parametric optimization and computational geometry. The work is partially supported by National Natural Science Foundation of China (60974042) and College Student Research Project Foundation of Zhejiang Province (G1401115042900).

Ju Zhang, Xinyan Cheng, and Jiaqi Zhu are with the Zhijiang College of Zhejiang University of Technology, No. 958, Kehua Rd, Keqiao District, Shaoxing, China (e-mails: zjk@zjut.edu.cn, {yewu1124, 731487737}@qq.com).
* Corresponding author.

ic property. The MPC system is difficult to be applied in problems with the short sampling time interval e.g., in the case of helicopter control, because on-line computation may not finish solving optimization problems in short sampling time intervals. In this paper, the Explicit Model Predictive Control (EMPC) approach for a 3-DOF helicopter is presented. By introducing Multi-Parametric Quadratic Programming (MPQP), explicit model predictive control moves the repeated online optimization computation to offline and provides an explicit optimal control law. The explicit model control law for current states can easily be obtained by searching the lookup table online.

Modelling of a 3-DOF helicopter and a state-space presentation is established in Section 2. The Explicit Model Predictive Control for a 3-DOF helicopter are calculated and the controllers for set-point regulation and tracking time-varying reference signals are presented respectively in Section 3. In Section 4, numerical study of EMPC for regulation and tracking problems are conducted. Finally, a hardware-in-the-loop study of explicit model predictive control is made.

2. MODELING OF 3-DOF HELICOPTER

As described in the free-body diagram of Fig. 1, 3-DOF (degrees-of-freedom) of a helicopter refers to the motion of elevation, pitch and travel axis. The arm is installed on an additional 2-DOF instrumented joint, which allows the helicopter body to move in the elevation and yaw directions. On one end of the arm are propellers, which are driven by two DC motors. When the voltage on each motor equals, the helicopter moves in an elevated direction. When unequal, the body pitches. Meanwhile, the thrust vectors result in travel of the body (i.e., yaw of the arm) as well. Encoders measure data from each degree of freedom. The other end of the arm carries a counterweight such that the effective mass of the helicopter is light enough for it to be lifted using the thrust from the motors. The vertical base is equipped with an eight-contact slip ring. Electrical signals to and from the arm and helicopter are channeled through the slip ring to eliminate tangled wires, reduce friction, and allow for unlimited and unhindered travel.

In deriving the dynamic model of the 3 DOF helicopter system, we assume that the changes of pitch and elevation are small, and that the helicopter system can be linearized approximately and relations among each degree of freedom is weak. Thus, the motion of each degree of freedom can be established separately.

Notice that the thrust forces$F_{\mathrm{f}}, F_{\mathrm{b}}$acting on the front and back motors are defined and made relative to the quiescent voltage V_{op}or operating point (equilibrium point).

$$V_{op} = \frac{1}{2}\frac{g(L_w m_w - L_a m_f - L_a m_b)}{L_a K_f}. \tag{1}$$

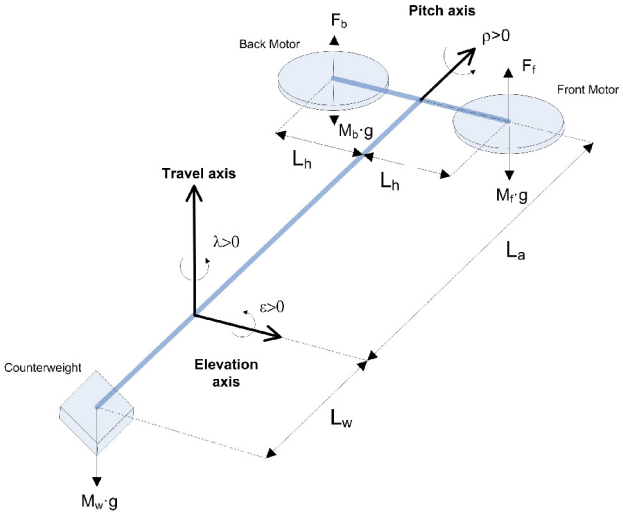

Fig. 1. The free-body diagram of 3-DOF Helicopter.

The parameters in (1) are defined in Table 1.

Remark 1: Here the equilibrium point is defined. The system status of the right part of the arm with motors in the horizon is defined as the equilibrium. Later in this article, all the system states (elevation angle, pitch angle and travel angle) are measured from this equilibrium.

Remark 2: In order to let the system stay at the equilibrium point, the quiescent voltage V_{op} as in (1) is needed. The actual voltage on the motor will be the sum of control voltage corresponding to controlU_f, $U_b$and the quiescent voltage V_{op}.

Remark 3: The quiescent voltage V_{op} is a constant and it is required because of the torque difference (effective gravity on elevation axis) between counterweight on the elevation axis and total mass of the two propeller assemblies on the elevation axis.

Remark 4: While rested on the laboratory table, the status of the system is not in equilibrium, but has a minus elevation angle, -27.5°, which will be considered as the initial condition in the regulation problem in section 3.

Remark 5: Some of the parameter values listed in Table 1 are obtained from the Quanser helicopter laboratory and user manual[7-8], some from the motor and encoder specifications, and some can be obtained through the experiments, e.g., the effective gravity $g(L_w m_w - L_a m_f - L_a m_b)$ on elevation axis can be measured with a scale.

2.1. Elevation

Considering the movement around the elevation axis in relation to equilibrium, and according to the free-body diagram in Fig. 1, it can be seen that only the torque generated by $F_m = F_{\mathrm{f}} + F_{\mathrm{b}}$ determines the movement around the

Table 1. System specifications.

Symbol	Description	Value
K_f	Propeller force-thrust constant	$0.1188N/V$
L_a	Distance between travel axis to helicopter	$0.660m$
L_w	Distance between travel axis to counterweight	$0.470m$
L_h	Distance between pitch axis to each motor	$0.178m$
T_g	Effective gravity on elevation axis	$T_g = m_t g L_a - m_w g L_w$
m_t	Total mass of two propeller assemblies	$m_t = m_f + m_b$
m_f, m_b	Mass of front/back propeller assembly	$m_f = m_b$ $(0.713kg)$
m_w	Mass of counterweight	$1.87kg$

elevation axis, and the following (2) can be established:

$$J_\varepsilon \ddot{\varepsilon} = (F_\mathrm{f} + F_\mathrm{b}) L_a = K_f (U_f + U_b) L_a, \tag{2}$$

Remark 6: Torques from effective gravity on the elevation axis T_g=$g(L_w m_w - L_a m_f - L_a m_b)$ do not appear in (2) because we are studying the movement in the vicinity of the equilibrium and the effects of T_g were already considered in the quiescent voltage as shown in (1) and in Remark 2 and Remark 3.

In (2), $\ddot{\varepsilon}$ is the elevation angular acceleration. U_f, U_b are control voltages applied to the front and back motors respectively to generate the thrust forces F_f, F_b. J_ε is the elevation rotary inertia. According to the mass distribution of the 3 DOF system with respect to the elevation axis shown in Fig. 1, J_ε is calculated the following way (neglecting the weight of the arm):

$$J_\varepsilon = m_f L_a^2 + m_b L_a^2 + m_w L_w^2 = m_t L_a^2 + m_w L_w^2,$$

where $m_t = m_f + m_b$, and following linear expression is obtained:

$$\ddot{\varepsilon} = \frac{K_f L_a (U_f + U_b)}{m_t L_a^2 + m_w L_w^2}. \tag{3}$$

2.2. Pitch

According to the free body diagram in Fig. 1, it can be seen that the pitch is caused by the difference between thrust forces generated by the front propeller and the back propeller respectively. If $F_f > F_b$, it will cause a positive pitch, otherwise, a negative pitch. It is easy to infer that the larger the pitch is, the more the helicopter will tilt and it is terribly uncomfortable for passengers in real cases.

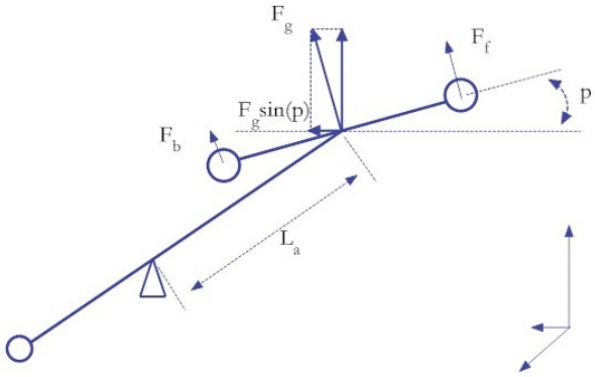

Fig. 2. Free-body diagram on travel axis.

The dynamics of pitch movement can be formulated as follows:

$$J_p \ddot{p} = (F_f - F_b) L_h = K_f (U_f - U_b) L_h, \tag{4}$$

In (4), $\ddot{p}$ is the pitch angular acceleration. $J_p$is the pitch rotary inertia. According to mass distribution of the system with respect to pitch axis shown in Fig. 1, J_p is calculated as follows:

$$J_p = 2 m_f L_h^2.$$

And then

$$\ddot{p} = \frac{K_f (U_f - U_b) L_h}{2 m_f L_h^2}. \tag{5}$$

2.3. Travel

If the body pitches, the thrust vectors result in a travel motion of the system as well. Therefore, it is a horizontal component of thrust forces $F_g \sin(p)$that makes the body travel.

The free-body diagram on travel axis is shown in Fig. 2. It is obvious that the more the body travels, the larger the distance of horizontal flight is.

The dynamic motion equation around the travel axis is described below:

$$\begin{aligned} J_\lambda \ddot{\lambda} &= L_a F_g \sin(p) = L_a (\mathrm{F}_f + \mathrm{F}_b) \sin(p) \\ &= L_a K_f (U_f + U_b) \sin(p). \end{aligned} \tag{6}$$

In (6), $\ddot{\lambda}$ is travel angular acceleration and p is pitch angle. J_λ is travel rotary inertia. According to mass distribution of the 3 DOF system with respect to the travel axis shown in Fig. 1,J_λ is calculated as follows (neglecting the weight of the arm):

$$\begin{aligned} J_\lambda &= m_f L_f^2 + m_b L_b^2 + m_w L_w^2, \\ L_f^2 &= L_b^2 = L_h^2 + L_a^2. \end{aligned}$$

It is assumed while considering the dynamics of travel motion that the dynamics of elevation can be ignored, i.e.,

$\ddot{\varepsilon} \approx 0$, making the force balance between the $F_g\cos(p)$ and the effective gravity on elevation axis. Thus, the approximation of (6) can be obtained as follows:

$$\begin{aligned}\ddot{\lambda} &= \frac{2L_aK_fV_{op}\sin(p)}{2m_fL_h^2+2m_fL_a^2+m_wL_w^2} \\ &= \frac{T_g\sin(p)}{2m_fL_h^2+2m_fL_a^2+m_wL_w^2}.\end{aligned} \tag{7}$$

When pitch angle p is small, $\sin(p) \approx p$ then the following linear expression(8) is obtained:

$$\ddot{\lambda} = -\frac{T_gp}{2m_fL_h^2+2m_fL_a^2+m_wL_w^2}, \tag{8}$$

where V_{op} is defined in (1), and $T_g = m_wgL_w - m_tgL_a$ is the effective gravity on elevation axis defined in Table 1.

Remark 7: From (8), it can be seen that if pitch keeps a constant nonzero angle p, the helicopter can do a rotation motion (travel motion) around the travel axis with constant acceleration.

Remark 8: Because of the multiply term, $\sin(p)$ and control U, (6) is a nonlinear differential equation, even if $\sin(p) \approx p$. It is very difficult to deal with (6) directly. Thus, it is necessary to make some approximation to simplify (6). The assumption of $\ddot{\varepsilon} \approx 0$ is reasonable while considering the dynamics of travel motion, which will be verified later in the control simulation experiment. Under this assumption, $F_g\cos(p) \approx F_g \approx 2K_fV_{op}$ (with small p).

Remark 9: According to (8), it can be seen that the control U_f, U_b will not directly affect the dynamics of travel motion. That is why the last low of matrix B at the end of this section will be zero. It can also be seen from (8) that the dynamics of travel motion is related to pitch angle p (this can also be seen from the nonzero element in the last low of system matrix A) and this is because there exists a coupling between the travel and pitch. Because the dynamics of pitch angle $p$is affected directly by control U_f, U_b, it can be understood that the dynamics of travel motion will be indirectly affected by control U_f, U_b. In deriving state space representation, system states, control inputs and output vectorare defined as follows:

$$x^T = [\varepsilon, p, \lambda, \dot{\varepsilon}, \dot{p}, \dot{\lambda}],\ u = [U_f, U_b]',\ y^T = [\varepsilon, p, \lambda],$$

where ε, p, λ are elevation angle, pitch angle and travel angle, respectively, measured from equilibrium, and ε, p, λ are their corresponding angular speeds.

According to the (3), (5), and (8), state space representation of the 3 DOF helicopter system can be established as follows:

$$\begin{bmatrix} \dot{\varepsilon} \\ \dot{p} \\ \dot{\lambda} \\ \ddot{\varepsilon} \\ \ddot{p} \\ \ddot{\lambda} \end{bmatrix} = A \begin{bmatrix} \varepsilon \\ p \\ \lambda \\ \dot{\varepsilon} \\ \dot{p} \\ \dot{\lambda} \end{bmatrix} + B \begin{bmatrix} U_f \\ U_b \end{bmatrix},$$

$$A = \begin{bmatrix} 0 & 0 & 0 & 1 & 0 & 0 \\ 0 & 0 & 0 & 0 & 1 & 0 \\ 0 & 0 & 0 & 0 & 0 & 1 \\ 0 & 0 & 0 & 0 & 0 & 0 \\ 0 & 0 & 0 & 0 & 0 & 0 \\ 0 & -1.2304 & 0 & 0 & 0 & 0 \end{bmatrix},$$

$$B = \begin{bmatrix} 0 & 0 \\ 0 & 0 \\ 0 & 0 \\ 0.0858 & 0.0858 \\ 0.5810 & -0.5810 \\ 0 & 0 \end{bmatrix}.$$

3. EXPLICIT MODEL PREDICTIVE CONTROL OF 3-DOF HELICOPTER

Due to the online repeated optimal computation, MPC is only applicable to systems of slow dynamics. To overcome the drawbacks of MPC, much research work has been done in order to shorten the online computation time, increase the online computation speed and broaden the application of MPC technologies [9-12]. Bemporad *et al.* [9] conducted breakthrough work in the field of explicit linear quadratic optimal control and Explicit Model Predictive Control (EMPC) by applying Multi-Parametric Quadratic Programming (MPQP) technologies to solve the quadratic optimal control problem. Based upon the MPQP technologies for the optimal control problem, state space is convexly partitioned and the implicit closed-loop MPC system can equivalently be transformed into an explicit Piece-Wise Affine (PWA) system. Therefore the explicit expression between optimal control sequence and states of the MPC system is obtained offline and there does not need solving the optimization problem online repeatedly.

3.1. Multi-parametric quadratic programming for constrained optimal control problem

In this section, the Multi-Parametric Quadratic Programming method for constrained optimal control problems and its main research results are summarized and are adopted to establish the EMPC for a 3-DOF helicopter system.

Considering the constrained optimal control problem:

$$J(U_N, x(0)) = ||Px_N||_2 + \sum_{k=0}^{N-1}(||Qx_k||_2 + ||Ru_k||_2), \tag{9a}$$

$$J^*(x(0)) = \min_{U_N} J(U_N, x(0)), \tag{9b}$$

$$\text{st.} \quad x_{k+1} = Ax_k + Bu_k, \quad k \geq 0, \tag{9c}$$

$$Ex_k + Lu_k \leq M, \ k = 0, \cdots, N-1, \tag{9d}$$

$$x_0 = x(0), x_N \in \chi_f, \tag{9e}$$

where U_N is optimal control sequence, $U_N = [u_0', \ ..., \ u_{N-1}']'$. Let $\chi \subseteq \Re^n$ to be the set of all feasible $x(0)$.

$x_N \in \chi_f$ is a final-state constraint region, χ_f is a convex set.

Remark 10: $P \geq 0$, $Q \geq 0$, $R \succ 0$, the reason is that we must penalize all the elements of the inputs so that it can be realizable in engineering practice. Some elements of the states, however, can be free, e.g. the speeds when emphasizing the positions.

Remark 11: Equation (9d) is the constraints for control input, states and outputs. The choice of the matrices E, L, M depends on the specific problem. In the 3-DOF control system case, the maximum control voltages on the motor must be constrained and the helicopter's motion scopes are also limited because of its placement in the laboratory table.

Because the controlled plant (9c) is linear, we have:

$$x_k = A^k x_0 + \sum_{j=0}^{k-1} A^j B u_{k-1-j}, \quad k = 1, \cdots, N. \tag{10}$$

Substituting (10) into (9a)-(9d), the constrained optimal control problem can be transformed into the following optimization problem (11)[9]

$$J^*(x(0)) = \frac{1}{2}x'(0)Yx(0) + \min_{U_N}\left(\frac{1}{2}U_N' H U_N + x'(0)F U_N\right),$$
$$\text{st. } GU_N \leq W + Ex(0). \tag{11}$$

The optimal control sequence $U_N^*(x(0))$ of (11) depends on its initial states $x(0)$. If the initial states $x(0)$ are considered as the parametric vector of the optimization problem (11) and the explicit relationship between $U_N^*(x(0))$ and $x(0)$ are established, the on-line repeated solution of optimization problem can be avoided. Based upon this idea, in literature [9], the optimization problem (11) is considered as Multi-Parametric Quadratic Programming (MPQP), and an algorithm for solving the MPQP problem is proposed. The explicit expression between $U_N^*(x(0))$ and$x(0)$ is obtained in the following (12)[9]:

For the MPQP problem (11), with$H > 0$, the feasible region χ is a convex set $\chi = \{x \in \Re^n | Lx \leq K\}$, and the optimal control sequence $U_N^*(x(0))$ is a Piece-Wise Affine (PWA) function of $x(0)$:

$$U_N^*(x(0)) = F^i x(0) + G^i \quad x(0) \in CR^i, \tag{12}$$

where CR^i are convex sets $CR^i = \{x \in \Re^n | L^i x \leq K^i\}$, and $\bigcup_i CR^i = \chi$ is a convex partition of χ, $CR^i \cap CR^j = \phi$ $(i \neq j)$, $(i, j = 1, ..., N^r)$, and N^r is the number of the states' region of the partition. The matrices L, K, F^i, G^i and L^i, K^i, N^r are obtained through solving the MPQP problem (11).

According to moving horizon strategy of the MPC system; in every discrete time instant, the control signal, which really acts on the plant, is the first element of $U_N^*(x(0))$, i.e., u_0^*. From (12), it is obvious that $u_0^*(x(0))$ is also a PWA function of $x(0)$. Therefore, for discrete time

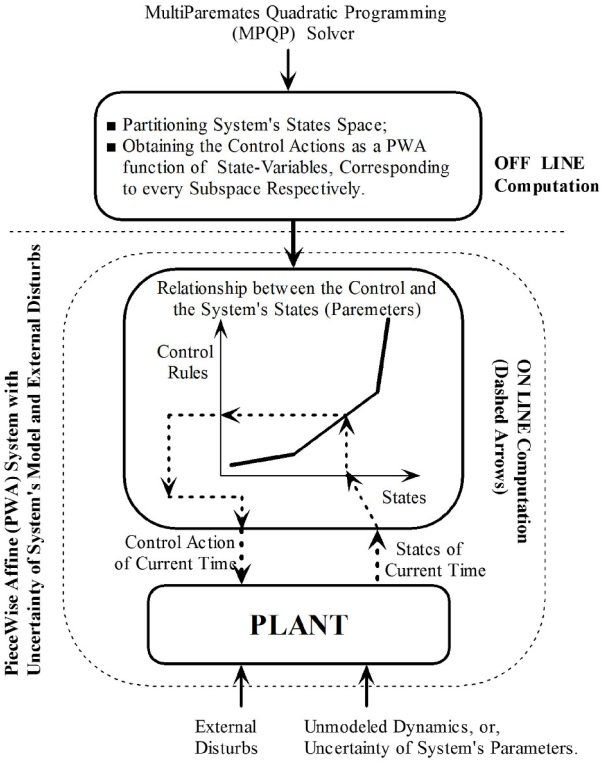

Fig. 3. Process of explicit model predictive control for a 3-DOF helicopter.

instant k and system states $x(k)$, the control signal $u(k)$ is a PWA function of $x(k)$:

$$u(k) = f^i x(k) + g^i \quad x(k) \in CR^i, \tag{13}$$

where f^i, g^i is the first low of F^i and G^i respectively.

With (13), the closed-loop MPC system can be equivalently transformed into a PWA system (14), which is the explicit MPC system.

$$\begin{cases} x(k+1) = (A + Bf^i)x(k) + Bg^i \\ y(k) = Cx(k), \end{cases} \quad x(k) \in CR^i. \tag{14}$$

The computations involved in the design and implementation of the explicit MPC system consist of two separate parts, i.e., the offline and online computation, as shown in Fig. 3 schematically.

During offline computation, by using the MPQP, the system states space is convexly partitioned, and the control laws as a PWA function of states are obtained. Over states region CR^i, the corresponding control law is the linear function of its states.

During online computation, the state region CR^i, in which the current states lie, i.e., $x(k) \in CR^i$, must be determined through the process of look-up table search. Then, the corresponding optimal control action for region $CR^i$is directly calculated according to $u(k) = f^i x(k) + g^i$.

3.2. Online computation

The majority of the online computational burden of model predictive control (MPC) has been removed by using multi-parametric programming, the so-called explicit MPC. The remaining online computation is only to determine the state region that the current state point lies in, through the process of the lookup table search.

The most direct solution is searching the polyhedral partitions sequentially to find out where the current state lies; the so-called, direct search method. The direct search method is simple and easy to implement.

A polytope can be defined as a bounded polyhedron. The polyhedron is the intersection of a finite set of half-spaces as follows:

$$CR^i = \left\{ x \in \Re^n \mid L^i x \leq K^i \right\}. \tag{15}$$

A convex polytope can also be defined with its vertices.

$$CR^i = \left\{ x \in \Re^n \mid x = \sum_i^{V_p} \alpha_i V_i^P, 0 \leq \alpha_i \leq 1, \sum_i^{V_p} \alpha_i = 1 \right\}. \tag{16}$$

After obtaining the current states $x(k)$, we look for their corresponding state region CR^i, such that $x(k) \in CR^i$. This can easily be done by substituting $x(k)$ into set definition (15) and checking if all inequalities are satisfied. If yes, $x(k)$ lies within this polytope. If either inequality is not satisfied, $x(k)$ does not lie in this polytope, and a search method must be applied to find out their corresponding CR^i.

Knowing how to determine if a point lies in a polytope, we can search through all state regions. In our case, we used the linear and sequential to search through the entire state region, one at a time, substituting $x(k)$ into set definition (10) until we find the state region that $x(k)$ lies in. If no state region is found, in the end, the control law of the nearest feasible region is used instead.

Linear search is easy to understand and realize. But as the scale and state regions increase, linear search will lose its advantage due to the large amount of computation. So, this is what many researchers are working on to improve online computation.

Once the current state is located in its corresponding region, the corresponding optimal control action is calculated according to (13). The process of the online computation is shown in the dashed arrows in Fig. 3.

Remark 12: For the 3-DOF helicopter system, an encoder is mounted for each degree of freedom. Therefore, the elevation angle, the pitch angle and the travel angle $[\varepsilon, p, \lambda]$ can be easily measured, and their corresponding speed $[\dot{\varepsilon},\ \dot{p},\ \dot{\lambda}]$ can be calculated through the derivative filter block. Therefore, the states $x(k)$ of the helicopter system can always be easily obtained at any time.

Remark 13: Direct search method is simple and easy to implement, and it is adopted in this work. When the number of the state regions is large, much time may be required performing online computations. To improve the online efficiency, several other methods have been proposed in literature. The reachability approach was proposed under the assumption that the next state point is near the current state point. A binary search tree and a flexible Piece-Wise function evaluation method were proposed for look-up table search [13, 14]. An orthogonal search tree was also used [15]. A two-stage algorithm, which combines the direct search method with the hash table, was proposed [16, 17]. The hash-based method enables the designer to tradeoff between online and offline computation complexity.

3.3. Explicit model predictive control of a 3-DOF helicopter

3.3.1 Regulation problem

For the regulation problem, the initial states are given: $x_0 = [-27.5°; 0; -13°; 0; 0; 0]$, with input and states constraints $|u| \leq 24(\mathrm{V})$, $x_{\min} = -[27.5°; 60°; 360°; 45(°/s); 45(°/s); 45(°/s)]$, $x_{\max} = [27.5°; 60°; 360°; 45(°/s); 45(°/s); 45(°/s)]$.

Q, R are both diagonal matrices. Q controls the performance of specific states, while R weighs the performance of control sequence. After many tries and simulations, the weighting matrices are chosen as $Q = \mathrm{diag}([100110002])$, $R = 0.05 * \mathrm{diag}([11])$.

For the regulation problem, discrete time Ts and prediction horizon$N$are chosen as $Ts = 0.5$s and $N = 1$. After the offline computation using MPQP, a state partition of 163 regions is obtained.

Remark 14: While rested on the laboratory table, the elevation angle is -27.5^o, and by moving the propellers of the helicopter; an arbitrary angle in travel can be set as the initial status. The constraints on voltage, angles and angular velocity come from the physical restrictions, moving limits in space and technical parameters of the helicopter system.

Remark 15: The weight matrices Q, R make it possible to tradeoff between the inputs and system performances. However, there exists no general law for the choice of values of Q, R. We have to resort to trial and error to obtain reasonable values.

Remark 16: For explicit model predictive control system, the number of state regions resulting from the MPQP problem will increase remarkably with increase of prediction horizon N and decrease of discrete time Ts. The overwhelming numbers of state regions will result in a cumbersome online lookup table search, and therefore have a negative influence on real-time performance and in some cases, deteriorating the control performances. However, theoretically, with smaller Ts and larger N, a better control performance will be obtained. Thus, there

exists a tradeoff among Ts, N, real-time and control performances. We prefer to choose large Ts and small N as much as possible on the premise that a satisfactory control performance is guaranteed.

3.3.2 Tracking problem

For the tracking problem; parameter settings including input and output constraints, weighting matrices Q and R, are same as that appear in the regulation control problem. The difference is the need for expanding state-space matrix. Additional reference state and previous input is added to original state vector, and the new input is:

$$\Delta u(k) = u(k) - u(k-1). \tag{17}$$

The state-space representation of attitude tracking is as follows:

$$\begin{pmatrix} x(k+1) \\ u(k) \\ x_{ref}(k+1) \end{pmatrix} = \begin{pmatrix} A & B & 0 \\ 0 & I & 0 \\ 0 & 0 & I \end{pmatrix} \begin{pmatrix} x(k) \\ u(k-1) \\ x_{ref}(k) \end{pmatrix} + \begin{pmatrix} B \\ I \\ 0 \end{pmatrix} \Delta u(k). \tag{18}$$

For the 3-DOF helicopter model with regards to the regulation problem, the size of matrix A is 6 by 6, while in the tracking problem (tracking $y^T = [\varepsilon, p, \lambda]$) the size of the augmented A is 11 by 11. Because of the augmented dimension, some adjustment for discrete sampling time and prediction horizon is needed.

To achieve optimum performance and fast online computation, $Ts = 0.5$, $N = 2$ are chosen. After the offline computation using MPQP, a state partition of 2453 regions is obtained. It is quite obvious that with the increasing dimension of the model, the number of regions rises rapidly. Thus, the explicit solution is ready for simulation and experiment.

4. NUMERICAL SIMULATIONS OF EXPLICIT MODEL PREDICTIVE CONTROL OF A 3-DOF HELICOPTER

In this section, numerical simulations of explicit model predictive control for regulation and tracking problems are conducted.

4.1. Regulation problem

Regulating the system from its initial states $x_0 = [-27.5;\ 0; -13; 0; 0; 0]$ to the equilibrium is shown in Fig. 4. It can be seen that the control results are satisfactory and almost the same, as we expected. There are no overshoots for elevation and travel trajectories. Although

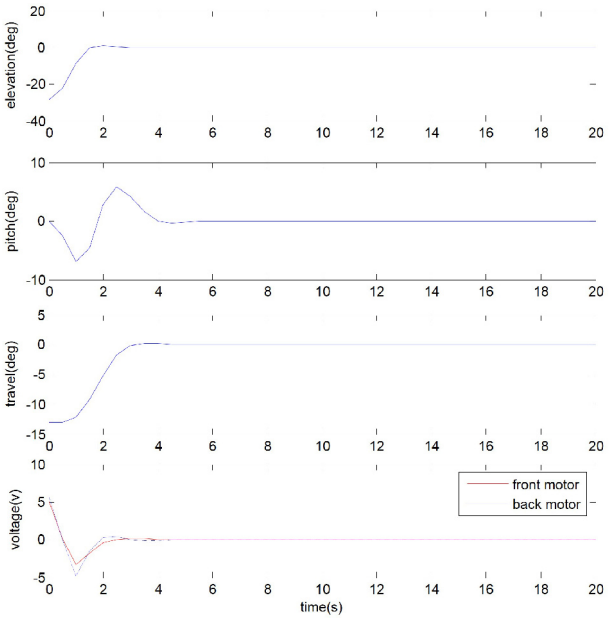

Fig. 4. EMPC regulation of a 3-DOF helicopter.

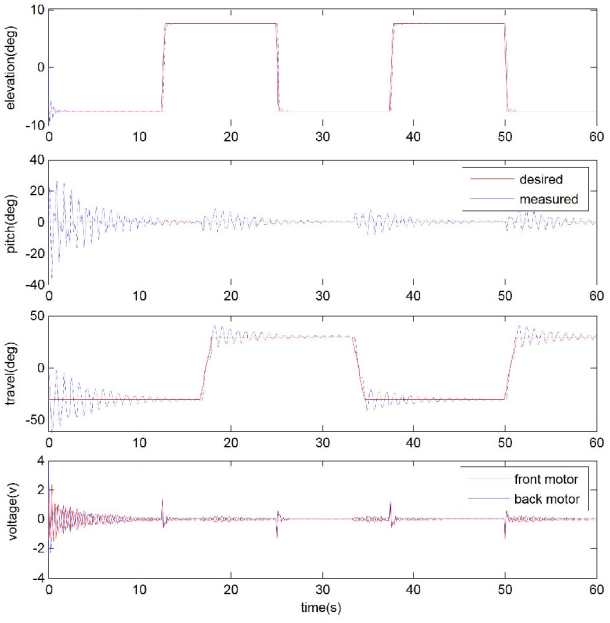

Fig. 5. EMPC tracking of 3 DOF helicopter.

the pitch angle has a zero initial value, it has a significant nonzero transient trajectory. It is because there exists a coupling between travel and pitch as noted in Remark 9.

4.2. Tracking problem

The simultaneous tracking of elevation square wave with amplitude 7.5 and frequency 0.04Hz, and travel

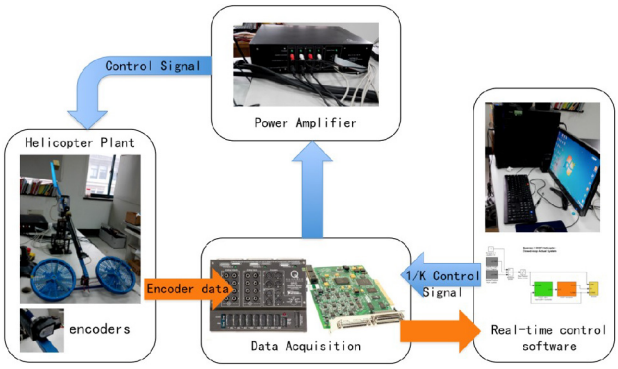

Fig. 6. HIL 3-DOF helicopter experimental system.

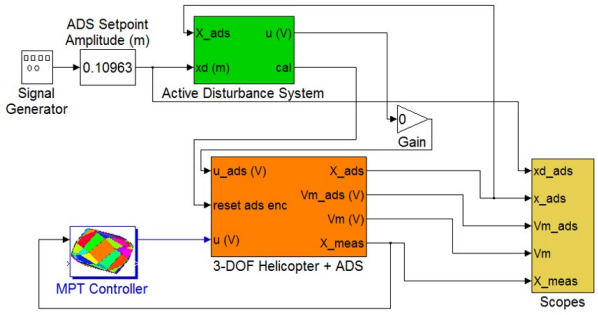

Fig. 7. Simulink diagram of HIL regulation.

square wave with amplitude 30 and frequency 0.03Hz are shown in Fig. 5.

It can be seen that for elevation square wave tracking, an almost perfect tracking performance is obtained, and for travel square wave tracking, a satisfactory performance is also demonstrated as we expected. It is obvious that there is a coupling between pitch and travel. It should also be noted that the voltages shown both in Fig. 4 and Fig. 5 are only the control voltages, which does not include the quiescent voltages V_{op} as discussed in the Remark 2.

It can be noted in Fig. 5 that the changes in control voltages occur significantly only during the moment when elevation changes. For the moment when travel changes, there is only small fluctuations in the control voltages and the control voltages are near zero. At the same time, there is no fluctuation of elevation resulting from the changes in travel. All these observations coincide with what discussed in Remark 8.

5. HARDWARE IN THE LOOP STUDY OF EXPLICIT MODEL PREDICTIVE CONTROL OF A 3-DOF HELICOPTER

In this section, a hardware (3-DOF helicopter) in the loop (HIL) experimental study of explicit model predictive control of 3-DOF helicopter is conducted. To analyze the dynamic performance of EMPC, a comparison is made with a PID controller for regulation and tracking square signals. Moreover, an Active Mass Disturbance System (ADS), which causes disturbance by moving the mass, is also added to examine the performances of an EMPC controlled helicopter system under disturbance.

As shown in Fig. 6, hardware in the loop experimental system of a 3-DOF helicopter consists of helicopter plant, data acquisition board, computer and power amplifier (with amplification coefficient of K). This HIL system is a real-time control experimental system with the support of real-time software QUARC. The orange arrows represent the acquisition of current states, while the blue arrows are actions of control solution. Encoders with resolutions of 4096 counts/revolution measure the pitch, elevation and travel angles. The controller is supervised by commands from a Matlab/Simulink based human machine interface. The hardware sampling frequency is set to 0.5 KHz.

5.1. Regulation problem

The Simulink diagram of HIL regulation experiment is shown in Fig. 7. The explicit model predictive controller is implemented in the block of MPT Controller. The input of the MPT controller is the current states of helicopter system and the output is the control voltages. The blocks of HIL Write Analog and HIL Read Encoder Timebase make it possible to connect seamlessly the MATLAB/Simulink with the data acquisition board and the 3-DOF helicopter system. The output of the MPT Controller, i.e., the control voltages for the front and back motors, is not applied directly to control the motor. A quiescent voltage V_{op} (equation (1)) is added to the original control voltages. As we have already mentioned in Remark 2, the thrust forces acting on the elevation, pitch, and travel axes from the front and back motors are defined and made relative to V_{op}. The Active Disturbance System (ADS) is also included in the Fig. 7, and by setting the corresponding value of Gain model the ADS system can be put into operation.

Experimental results of regulations from initial states $x_0 = [-27.5; 0; -13; 0; 0; 0]$ to equilibrium are shown Fig. 8.

Both the results of EMPC regulations and PID regulations are presented for comparison. Note the different scales of the vertical coordinates in Fig. 8(a) and Fig. 8(b). It can be seen that the EMPC regulation exhibits a better performance than that of PID.

For PID scheme, there is an obvious overshoot, and there also exists large fluctuation of pitch and great varying range of voltages in the early transient period. For EMPC scheme, admittedly, there is a fluctuation of the pitch in the long period of the regulating process and the control voltage exhibits some burrs. Although regulation using EMPC responds a little slower than that of using PID, the maximum offset of EMPC is much smaller than that of using PID. Besides, EMPC settles faster.

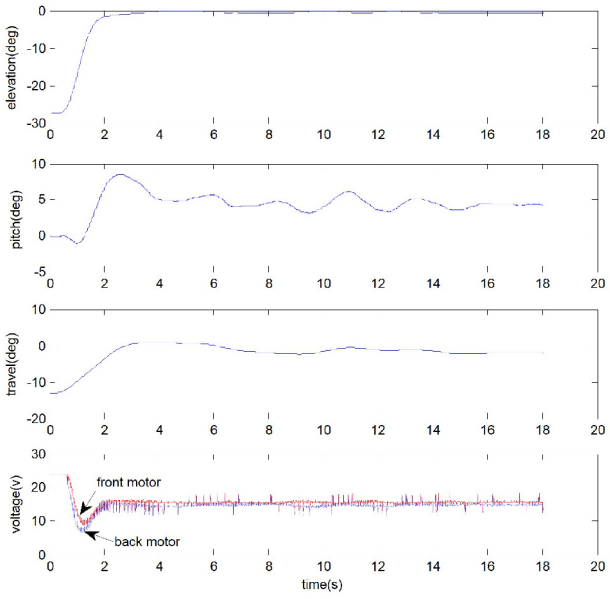

(a)

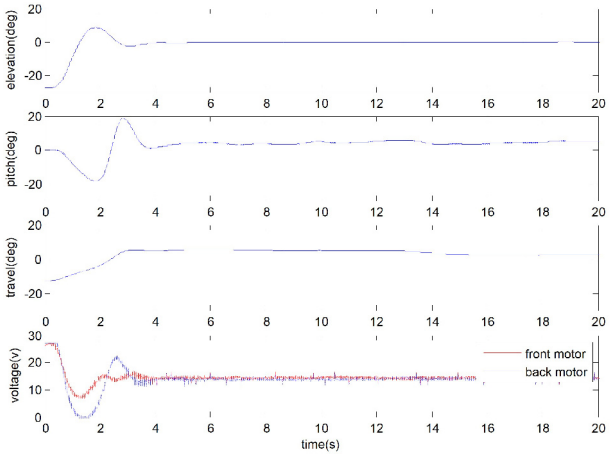

(b)

Fig. 8. (a) Experiment results of EMPC regulations, and (b) Experiment results of PID regulations.

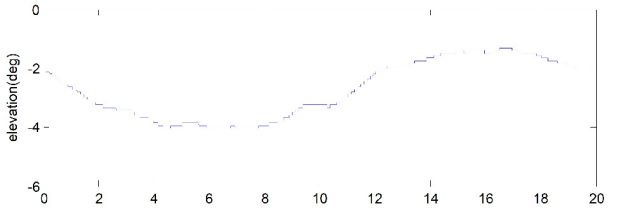

Fig. 9. EMPC Regulation of a 3-DOF Helicopter with Active Mass Disturbance.

5.1.1 Regulation with Active Mass Disturbance

Active Mass Disturbance System (ADS) consists of a lead-screw, a DC motor, an encoder, and a moving mass.

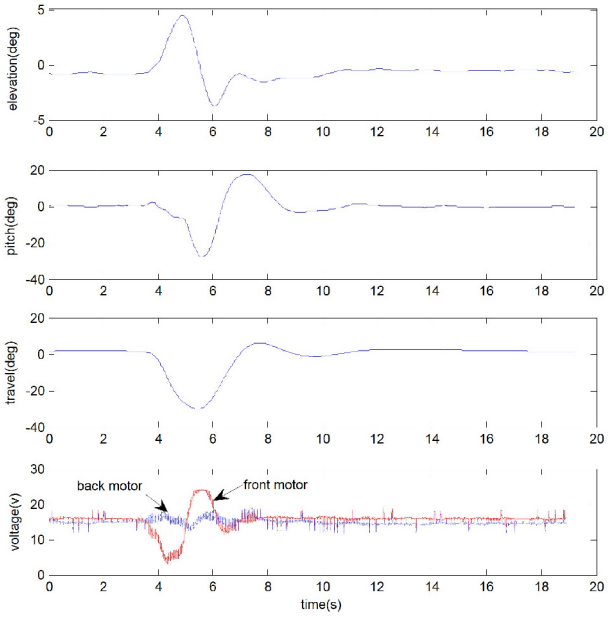

Fig. 10. EMPC regulation with manual interference.

The lead-screw is wound through the mass such that when the lead is rotated, the mass moves along the helicopter arm linearly. The lead-screw is 0.264m long and its pitch is 1/3 in/rev. One end of the lead-screw is rotated and causes the mass to move. Using the encoder measurement and a position controller, the mass can be moved to a desired position and actively disturb the helicopter. In this paper, the mass moves according to a sinusoidal signal whose amplitude is 0.10963m and frequency is 0.05HZ.

After the helicopter is regulated to equilibrium by EMPC, the ADS begins to work by turning the value of the Gain model in Fig. 7 to 1. Fig. 9 shows the elevation trajectory with the working of ADS.

Remark 17: Although the persistent disturbances were not considered explicitly in the EMPC controller synthesis, it can be seen that for the persistent disturbance of ADS, the performance of elevation trajectory is acceptable with small fluctuation around its equilibrium.

5.1.2 Regulation with manual interference

Fig. 10 shows their regulating trajectory after providing a manual disturbance such that elevation angle and travel angle are deviated from their equilibrium simultaneously. After a short time period of adjustments, the system can come back to its equilibrium again with satisfactory performance.

Remark 18: From above 2 kinds of regulation problems with disturbances, it can be seen that the EMPC scheme for a 3-DOF helicopter system exhibits some of the extent of its anti-disturbance abilities.

Remark 19: The ADS system can be understood as

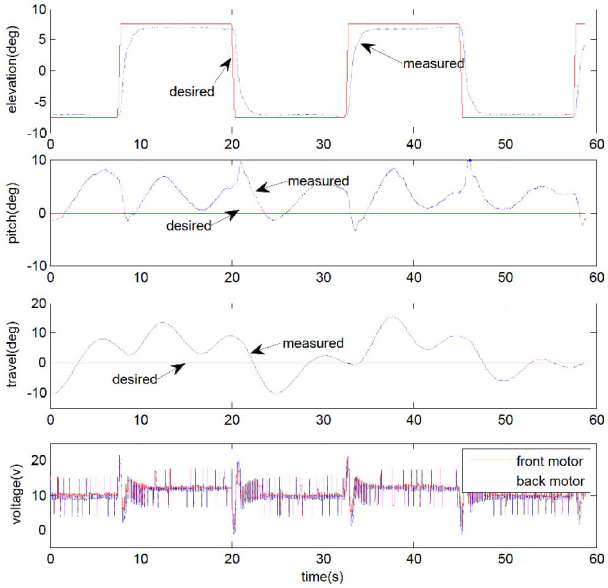

(a)

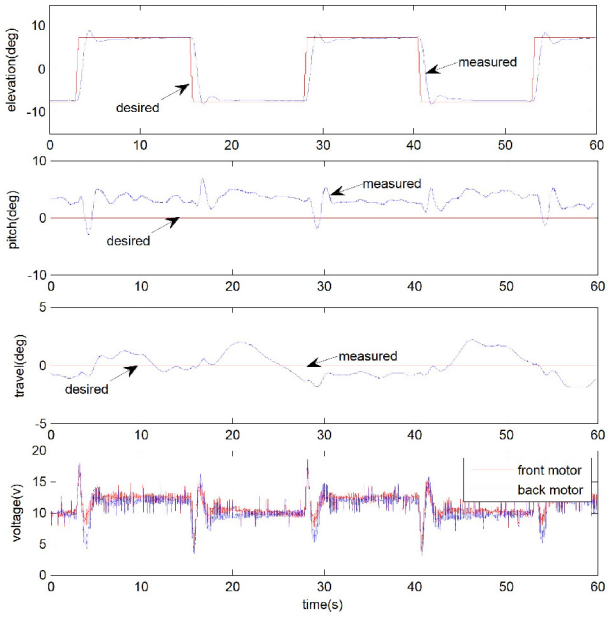

(b)

Fig. 11. (a) Experiment results of EMPC elevation tracking, and (b) Experiment results of PID elevation tracking.

some kinds of persisting disturbances, e.g. the external winds and air turbulence, or the parameter uncertainty of the system. Manual interference can be viewed as the analog of some impulse disturbances, e.g. wind gust and abrupt load or unload for helicopter.

5.2. Tracking problem

The experimental results of elevation tracking of a square wave with amplitude of 7.5 degrees and frequency of 0.04Hz are shown Fig. 11. Both the experiment results of EMPC elevation tracking and PID elevation tracking are presented.

It can be seen that for elevation movement, the EMPC regulation exhibits a little bit better performance (no overshoot and less delay in tracking) than that of PID. Although no reference signals are given for pitch and travel movement, there are significant responses in these motions for both control schemes. This is because of the coupling of the movements and the nonzero initial conditions in these 2 degrees of freedom.

Remark 20: Although the EMPC scheme exhibits a satisfactory tracking performance for a specific reference signal, the tracking problem is usually more difficult and complicated than the regulating problem, both in terms of design and implementation because of the augmented dimension for tracking in an EMPC scheme. Thus, EMPC seems more suitable for the regulating problem.

Remark 21: By Comparison of the EMPC experimental results with the simulation results and PID scheme, it shows a satisfactory control performance of the EMPC controller and the validity of the developed control model.

6. CONCLUSIONS

In this paper, an explicit model predictive control approach for the Quanser 3-DOF helicopter system is studied. The models of the 3-DOF helicopter system are developed, and EMPC regulation controller and tracking controller are synthesized. Numerical simulations and hardware-in-the-loop (HIL) experimental studies are made. EMPC approach is compared with the PID scheme while controlling the helicopter system. An Active Mass Disturbance system and manual disturbances are also considered. This research work shows that the explicit model predictive control is valid for application in a 3-DOF helicopter system.

REFERENCES

[1] A. T. Kutay, *et al.*, "Experimental results on adaptive output feedback control using a laboratory model helicopter," *IEEE Transactions on Control Systems Technology*, vol. 13, no. 2, pp. 196-202, March 2005. [click]

[2] B. Zheng and Y. Zhong, "Robust attitude regulation of a 3-DOF helicopter benchmark- theory and experiments," *IEEE Transactions on Industrial Electronics*, vol. 58, no. 2, pp. 660-670, March 2011. [click]

[3] M. Ishitobi, M. Nishi, and M. Miyachi, "Nonlinear model following control with parameter identification for a 3-DOF model helicopter," *Proc. of IEEE/ASME International Conf. Advanced Intelligent Mechatronics*, pp. 1-6, 2007. [click]

[4] I. Postlethwaite, I. Prempain, E. Turkoglu, C. M. Tuner, K. Ekkis, and A. W. Gubbels, "Design and flight testing of

various h-infinity controllers for the Bell 205 helicopter," *Control Engineering Practice*, vol. 13, no. 3, pp. 383–398,March 2005. [click]

[5] H. Sira-Ramirez, M. Zribi, and S. Ahmad, "Dynamical sliding mode control approach for vertical flight regulation in helicopters," *IEEE Proceeding Control Theory and Application*, pp. 19–24, 1994. [click]

[6] M. Morari and J. H. Lee, "Model predictive control: past, present and future," *Computers & Chemical Engineering*, vol. 23, no. 4-5, pp. 667–68, May 1999. [click]

[7] Quanser Inc., *3-DOF Helicopter Laboratory Manual*, 2011.

[8] Quanser Inc., *3-DOF Helicopter User Manual*, 2011.

[9] A. Bemporad, M. Morari, V. Dua, and E. N. Pistikopoulos, "The explicit linear quadratic regulator for constrained systems," *Automatica*, vol. 38, no. 1, pp. 3–20, January 2002. [click]

[10] M. T. Cychowski and K. Szabat, "Efficient real-time model predictive control of the drive system with elastic transmission," *Control Theory & Applications, IET*, vol. 4, no. 1, pp.37-49, January 2010. [click]

[11] A. Grancharova and T. A. Johansen, "Design and comparison of explicit model predictive controllers for an electropneumatic clutch actuator using On/Off valves," *IEEE/ASME Transactions on Mechatronics,* vol. 16, no. 4, pp. 665-673, August 2011. [click]

[12] C. Panos, K. I. Kouramas, M. C. Georgiadis, and E. N. Pistikopoulos, "Modelling and explicit model predictive control for PEM fuel cell systems," *Chemical Engineering Science*, Vol. 7, no. 1, pp. 15-25, January 2012. [click]

[13] P. T∅ndel, T. A. Johansen, and A. Bemporad, "Evaluation of piece wise affine control via binary search tree," *Automatica*, vol. 39, pp. 743–749, May 2003. [click]

[14] F. Bayat, T. A. Johansen, and A. A. Jalali, "Flexible piecewise function evaluation methods based on truncated binary search trees and lattice representation in explicit MPC," *IEEE Transactions on Control System Technology*, vol. 20, no. 3, pp. 632-640, April 2012. [click]

[15] T. A. Johansen and A. Grancharova, "Approximate explicit constrained linear model predictive control via orthogonal search tree," *IEEE Transactions on Automatic Control*, vol. 48, no. 5, pp. 810–815, May 2003. [click]

[16] A. N. Fuchs, C. N. Jones, and M. Morari, "Optimized decision trees for point location in polytopic data sets application to explicit MPC," *Proc. of American Control Conference*, pp. 5507-5512, 2010. [click]

[17] F. Bayat, T. A. Johansen, and A. A. Jalali, "Using hash tables to manage the time-storage complexity in a point location problem: Application to explicit model predictive control," *Automatica*, vol. 47, no. 3. pp. 571–577, 2011. [click]

Ju Zhang obtained his B.S. degree in Mechanical Engineering from Zhejiang University of Technology in 1994, and his Ph.D. degree in Automatic Control Engineering from Zhejiang University in 2005. From 2005 to 2006, he was a visiting scholar at Stuttgart University, Germany. From 2007 to 2010, he was an associate Professor, and from 2011, he is a Professor, both at college of information Engineering, Zhejiang University of Technology. From 2014 to 2015, he was a visiting scholar at Michigan State University, USA. His research interests are in the areas of model predictive control, hybrid system and linear parameter varying systems.

Xinyan Cheng obtained her B.S. degree in Measuring and Control Technology and Instrumentations from China Jiliang University in 2008 and her M.S. degree in Automatic Control Engineering from Zhejiang University of Technology in 2015. Her research interests include explicit MPC control and helicopter control.

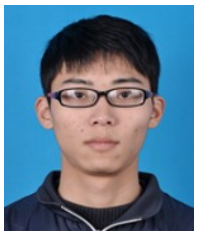

Jiaqi Zhu obtained his B.S. degree in Automatic Control Engineering from Zhejiang University of Technology in 2015. His research interests include explicit MPC.